Experimental analysis of recoil effects induced by fluorescence photons

Alexander Zhdanov,[1] Satish Rao,[2] Andrey Fedyanin,[1] and Dmitri Petrov[2,3]
[1]*Faculty of Physics, M.V. Lomonosov Moscow State University, Moscow 119991, Russia*
[2]*ICFO-Institut de Ciencies Fotoniques, Mediterranean Technology Park, 08860 Castelldefels, Barcelona, Spain*
[3]*Institució Catalana de Recerca i Estudis Avançats (ICREA), 08010 Barcelona, Spain*
(Received 20 April 2009; published 6 October 2009)

The momentum transfer to a scatterer from fluorescence photons was detected using an optical system that permits one to simultaneously measure the radiation force exerted on and fluorescence emission from the scatterer. The core of this technique is a partially metal covered dielectric bead optically trapped in a liquid with dye molecules. Fluorescence emission from the volume that includes the bead is measured simultaneously with the Brownian motion of the bead. The perturbed motion of the bead is a result of photon momentum transfer from the fluorescence of the dye to the trapped scatterer. The bead position fluctuations indicate the presence of the fluorescence and its bleaching nature. The results demonstrate the capability of the photonic force microscopy technique to be a complement to spectroscopy in the study of optical processes.

DOI: 10.1103/PhysRevE.80.046602 PACS number(s): 42.50.Wk, 87.80.Cc, 87.64.kv

I. INTRODUCTION

Fluorescence and Raman processes, where a material absorbs and emits light at different wavelengths, are widely used for both fundamental studies and applications. The conventional way to characterize these effects is through the analysis of a spectrum of light reflected from a scatterer. However, one can consider a different physical perspective where the fluorescence and Raman scattering result in a change in the total scattering field due to the emission of the photons. Any changes in the total scattering field by a given incident field induces mechanical forces that are exerted on the scatterer [1,2]. The inelastic processes that are included in the light-matter interaction also contain a momentum exchange between the incident and scattered photons and the scatterer; therefore, a measure of the radiation forces acting on the scatterer is equivalent to the measurement of its recoil that is exerted by the photons. This general idea has been pursued previously for two cases that are not related with emission processes: an additional radiation pressure on optically levitated (or trapped) dielectric spheres attributed to Mie resonances [3,4] and an absorption-induced radiation pressure in a dielectric sphere doped by dye molecules [5].

Recently, we measured the effects related with the momentum transfer of emitted Raman photons in the near infrared range [6]. We employed photonic force microscopy (PFM) coupled with Raman detection to simultaneously measure the radiation forces exerted on and the Raman emission from a micron-sized scatterer optically trapped in a liquid by a focused beam which also excites the Raman scattering. The results showed that the PFM with our scatterer (a dielectric bead partially covered by metal) was sensitive enough to detect the momentum transfer from the emitted Raman photons to the scatterer through detection of the nanometer movement of the scatterer. The correlation of these processes offers an alternative measure to the Raman emission output. The results led to the belief that such a technique could be applied to other light processes.

The goal of the present study is to expand this idea to fluorescence processes, in particular, to study the recoil effect as a result of the fluorescence of dye molecules that are proximal to or adsorbed on the surface of an optically trapped probe. We aim to show that in addition to a response to the fluorescence photon momentum transfer, the scatterer can track known fluorescence effects. The example that will be demonstrated here is photobleaching. This is a natural extension of our previous work; however, considerable changes to the optical setup are required due to the strong bleaching processes in dyes, which are further explained below. In order to increase the efficiency of the fluorescence process the scattering probe contains nanosized metal colloids that enhance the emission through surface-enhanced fluorescence (SEF) (for example, [7]). SEF phenomena originate from localized surface plasmon resonances in nanoscopically textured metal structures that lead to large enhancements of the fluorescence efficiency. The effect is pronounced because the field enhancement occurs twice. Initially, the collective oscillations of local surface plasmons radiate coherent light that is resonant with the excitation. The increased fluorescence scattering is further magnified by the same mechanism resulting in a higher total output. This phenomenon mimics that of surface-enhanced Raman scattering (SERS) which was utilized in our previous study of the momentum transfer from Raman photons [6].

The principal idea of our measurements is the following. A scatterer, which acts as the probe, is a micron-sized dielectric sphere partially covered by nanosized metal colloids. A focused optical beam (trapping beam) traps the probe in a liquid medium with dye molecules so that its Brownian motion is confined near the focus. Another beam (pump beam) with wavelength close to the maximum absorption of the dye is introduced coaxially with the trapping beam. Hence, dye molecules in close proximity to the surface of the scatterer are excited and consequently their emission is enhanced through the SEF process. Previous studies have shown enhancement from molecules stuck to the metal surfaces [8] up to molecule-metal distances of tens of nanometers [9]. The momentary position of the probe is analyzed by the measurement of the forward scattered light of a third beam (position detection beam) propagating coaxially to the trapping and pump beams. The intensity of the position detection beam is

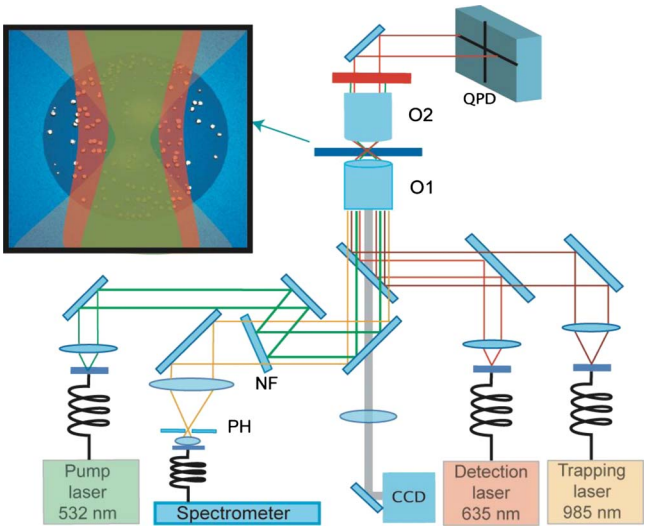

FIG. 1. (Color online) A schematic of the experimental setup with a drawing (inset) of the optically trapped metal covered bead illuminated by the trapping, pump, and position detection beams.

weak enough such that it does not significantly affect the stiffness of the trap nor the fluorescence spectra and hence, trapping, position, and excitation become independent operations. The position of the probe is statistically found with the average value being the sum of two random processes: Brownian motion with a known (white) spectrum of the random force and SEF—another process with sporadic fluctuations due to not completely known mechanisms of interaction between the molecules and metal [10]. Thus, the simultaneous collection of the probe motion and emitted fluorescence allows for a direct comparison and correlation between the two observables.

The synthesis of the probe is also an important consideration. Nanosized metal spheres are excellent field enhancers, however, trapping them can be complicated due to the increased scattering forces arising from their highly reflected surfaces [11–13]. We counter this problem by using a dielectric sphere that is partially covered with nanofeatured silver colloids. A low partial coverage can be achieved that allows the sphere optical trapping while still having enough metal to produce detectable enhanced fields [14–16]. The metallized surface should be roughened [17] and in the case of silver have island dimensions of around 100 nm [18]. This provides a high scattering cross section and depending on the surface topography can lead to high field enhancement for particles in close proximity.

II. EXPERIMENTAL METHODS

A. Setup and sample preparation

The probes are 2 μm in diameter silica beads that are partially covered by silver colloids [19] prepared by the citrate reduction method [20]. The silver colloids varied in diameter between 50–100 nm with a peak size of about 70 nm (Fig. 1 inset). The beads were prepared by attaching silver colloids to silica spheres via a self-assembling silane monolayer using slight modifications of the methods from [16,20]. The colloid sizes were confirmed by scanning electron microscopy (SEM) and absorption spectroscopy (image and plot not shown). The colloid coverage of the sphere surface was about 10% which we found to be optimal for both trapping and SEF. SEM imaging confirms a homogeneous metal coverage. This is expected when considering the colloid intrinsic charge that forces consistent separation between neighbors at reasonable concentrations.

Samples were prepared by mixing beads with Rhodamine 6G (R6G) in water with a final dye concentration of 3×10^{-7} M with an addition of a minute amount of 0.01 M NaCl. R6G was chosen because it has strong SEF activity [21], is soluble in water which eases its incorporation with the beads, and there is a common understanding of its fluorescence spectrum.

Figure 1 is a schematic of the setup used. A beam from a CW 985 nm laser produced the trapping beam with a variable stiffness. The field distribution near the focal spot of a high numerical aperture lens dictates the trap stiffness to be inherently smaller in the beam propagation direction (z) than in the perpendicular directions (x and y) allowing for a higher force sensitivity in the z direction. Thus, for sufficiently small forces, such as those observed here, the z force component of the trapped probe will give the most consistent information.

To excite the luminescence of R6G molecules a second CW 532 nm beam was introduced along with the trapping beam through a notch filter and a dichroic mirror. The diameter of this beam at the focal plane is around 1 μm. The backscattered emission of the R6G molecules was collected by the trapping objective and then passed through the notch filter and a confocal system (300 μm confocal pinhole) before arriving at a spectrometer.

We analyzed the probe position fluctuations with a position detector. For these measurements a third 633 nm beam was introduced along the trapping and pump beam with its intensity so low that it did not interfere with the 985 nm trapping. The forward scattered 633 nm light from the sphere trapped by the 985 nm beam was collected by a 40× objective (O_2) and passed to a quadrant photodetector (QPD). The measurement of the stiffness of the trap was based on established theory of Brownian motion of a particle in a confining potential [22]. In order to evaluate the linear range of the QPD, and to calibrate it, a sphere stuck to the cover slip was translated by a known distance through the detection beam spot. The linear range was approximately ± 500 nm for the x and y directions and ± 400 nm for the z direction.

Data collection was conducted with a LABVIEW platform based software that acquired synchronously the data from the spectrometer and the position detector. Thus, the fluorescence spectra and the probe position fluctuations were obtained with a desirable time resolution. Individual fluorescence spectra were recorded with a 1 s acquisition time while the position data were collected at a fast enough rate to be considered continuous.

B. Optical trapping dynamics

Our measurement uses the equilibrium position of the optically trapped probe in the absence of the pump beam as the

reference point. When the pump is on, luminescence emission from molecules in the proximity of or adsorbed on the metal surfaces is measured along with the corresponding photon momentum transfer which is detected through the measurement of the new probe position.

The propagating pump beam will undoubtedly destabilize the trap due to the additional scattering force. We try to counter this by reducing the beam's filling of the objective back aperture and keeping its focus as close to the trap beam focus as possible. Control experiments, a plain and metal covered bead in water only, assure that the bead remains at a stable position in the trap at constant pump power.

The use of separate beams for trap and pump, which differs from the method used in [6], is essential in order to keep the pump beam at a low intensity such that the bleaching processes of the dye are slowed. We could also, as shown below, vary the pump intensity at a given value of the trapping power. Although the pump power does not exceed several mW, thermal effects cannot be completely thrown out yet because the 532 nm wavelength is near the maximum absorption for the silver nanoparticles of 100 nm in size.

In order to calibrate the 985 nm trap, i.e., to determine the trap stiffnesses, we first collected the position fluctuations for the bead in water. The resulting histograms indicate full widths at half maximum of 100 nm and 150 nm for the x and z axes, respectively. A power spectrum density of the fluctuations was fitted and trap stiffnesses were extracted using an established method [22].

III. RESULTS

The pump beam not only excites the fluorescence of the molecules on or near the metal surfaces, which induces the recoil, but also exerts its own radiation force on the probe. This radiation force contains two contributions: scattering/gradient forces and metal colloid absorption at the bead´s surface. In order to understand the effect of the pump beam alone, we measured the displacement of a plain silica sphere (SS) and of the probe, a silica sphere partially covered by silver (SCS), both optically trapped in water without dye molecules as a function of pump power.

Figure 2 shows the z coordinate of the trapped SS as a function of time. At each interval the pump beam is turned on at a higher power than the previous one with the gaps at 0 nm indicating that the pump beam is blocked while its power is changed. For higher powers the pump beam not only shifts the equilibrium position of the probe along the optical axis but also increases the trap stiffness causing the narrowing of the position distribution. For the calibration of the position detection system we used the traces of the probe position obtained without the pump beam (time interval 220–320 s). The same experiment was performed with SCS spheres (data not shown) and data similar to Fig. 2 were observed with no significant difference seen in the histograms of the confined Brownian motions between the SS and SCS spheres in the absence of the pump beam.

Figure 3 shows the axial force F_z exerted on the scatterer as a function of the pump intensity both for SS and SCS in water. As seen, for the SS the force grows linearly with the pump intensity but the SCS shifts are larger than those of the SS at each pump intensity.

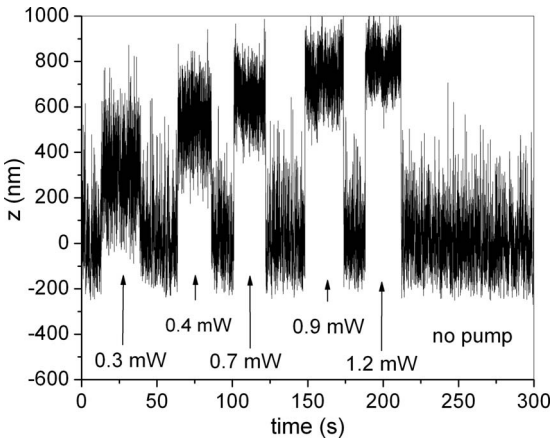

FIG. 2. Position data (z axis) of the SS trapped in water (no dye) over time while increasing pump power at certain intervals. The pump beam is blocked for some time before increasing the power to the next level. The positive value of z corresponds to the shift of the probe position along the propagation direction of the trapping beam.

Figure 4 contains the temporal behavior of the force on SCS in water in the presence of the pump. This figure shows that without dye molecules in solution the force is only dependent on the pump power and remains constant at constant pump power. For this and the following plots, the continuous position fluctuation data, represented as a force, are adjacent point averaged for clarity.

Figure 5 (inset) demonstrates fluorescence spectra that are detected in the absence and presence of a trapped SCS in dye solution. The main curve is the resulting difference spectrum. The fluorescence intensity increases about 20% in the presence of SCS in spite of the fact that the dye molecules are expelled from the confocal volume with the sphere in the center. This is an indication of the emission field enhancement.

To study this phenomenon more closely, we reduce each fluorescence spectrum to a single point by integrating over the wavelength region where strong fluorescence occurs

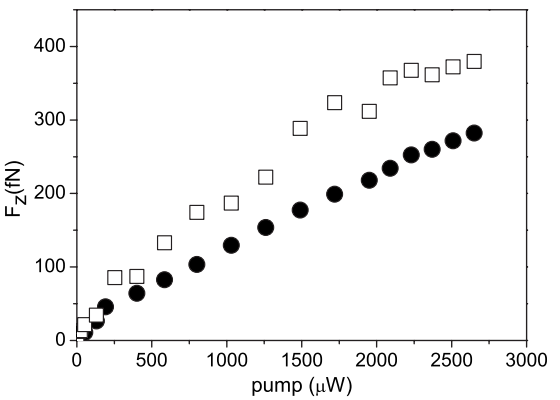

FIG. 3. Force values (z axis) acting on the SS and SCS trapped in water (no dye) under varying pump powers. Each point is the result of averaging of 20 probe position measurements during 1 s. Errors bars are about the size of the symbols.

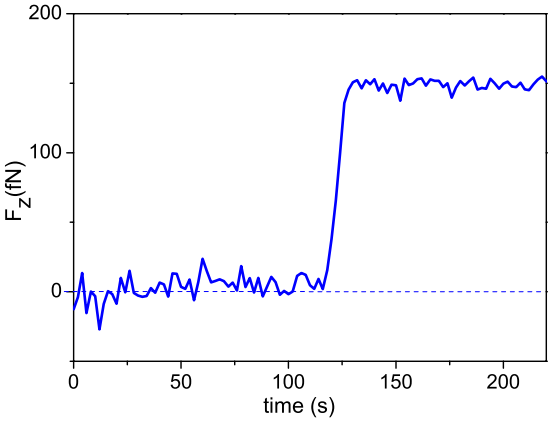

FIG. 4. (Color online) Force acting on the SCS trapped in water (no dye) without the pump (time interval $0<t<125$ s) and at the pump 0.8 mW ($t>125$ s).

(540–600 nm). The integration of the total measured fluorescence is what is used as the measure to track the emission over time, which is plotted in the following figures. The difference spectrum indicates a wavelength-dependent enhancement of the fluorescence intensity in the presence of the SCS (Fig. 5) which we observed previously when studying the field distribution near the SCS [23].

Next, we conducted the correlated force-fluorescence measurements in the presence of dye molecules. Figures 6 and 7 are plots of the integrated fluorescence and bead position fluctuations for the same constant pump power (50 μW) for the SS and SCS, respectively. A low pump power is used in order to study the regime with minimal to no bleaching effects.

To ensure that the perturbed bead movement is not a result of spurious effects, data for an SCS stuck to the glass cover slip, thus stopping its motion, were collected in the presence of the dye. Although SEF was still observed, the position fluctuations measured were only those that are characteristic of electronic systems noise and variation in the detection laser intensity. Thus, the position detection beam can be assumed to have no effect on the SEF-QPD correlations.

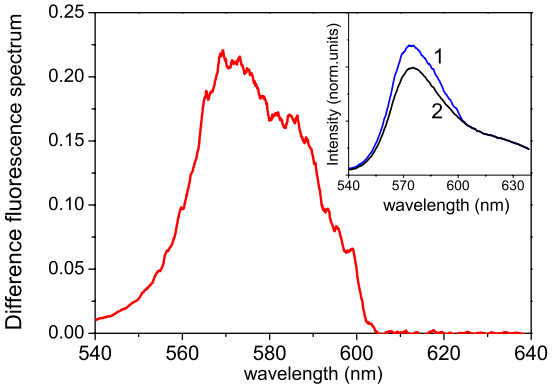

FIG. 5. (Color online) Fluorescence difference spectrum obtained with an SCS trapped in dye solution in the confocal volume. The spectrum is the difference between the measured fluorescence in the presence (curve 1 inset) and absence (curve 2 inset) of the trapped SCS. The pump is 0.02 mW.

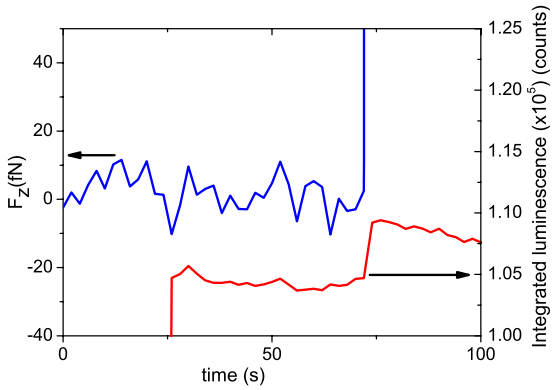

FIG. 6. (Color online) Integrated fluorescence (right axis, red line) of dye solution with a trapped SS plotted with the measured force z (left axis, blue line) on the bead over time. The pump beam is first off ($t<25$ s), then turned on (50 μW) ($25<t<75$ s) before the bead is expelled from the trap by blocking the trap beam ($t>75$ s).

The experiment is then moved to the high power regime where bleaching effects are expected. This is demonstrated in Fig. 8 where the pump power is varied over time. We used a specific protocol for increasing the pump power; most notably, the high enhancement of the incident field and the efficiency of the dye necessitated a slow increase in the pump power to avoid ejecting the bead from the trap. The slow increase allows for some photobleaching to occur which limits the maximum emitted fluorescence, and thus maximum applied force, at each power level. From 0–17 s the pump power is 0.13 mW. The power is then gradually increased until it reaches 0.8 mW at 28 s. The power remains constant until at 95 s when it is increased to 1.3 mW and is held at this value until the end of the measurement. Steps in the z position are still observed with the pump power increase; however, bleaching effects are also seen.

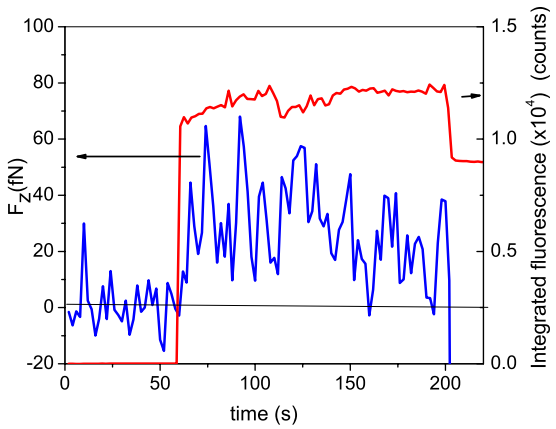

FIG. 7. (Color online) Low-pump power response. The pump power is 50 μW. Integrated fluorescence (right axis, red line) of dye solution with a trapped SCS plotted with the measured force (left axis, blue line) over time. The pump beam is first off ($0<t<60$ s), no luminescence is observed, and the average bead position is assigned to 0. During $60<t<200$ s the pump beam is on. At $t>200$ s the trapping beam is off and the fluorescence signal corresponds to the emission of the dye molecules in the confocal volume.

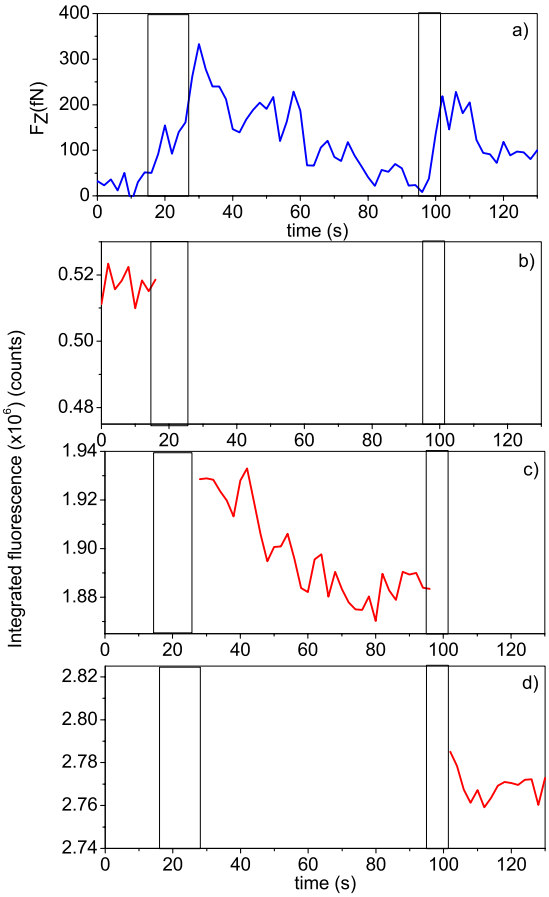

FIG. 8. (Color online) High-pump power response. From 0–17 s the pump power is 0.13 mW. The power is then gradually increased until it reaches 0.8 mW at 28 s. The power remains constant until at 95 s when it is increased to 1.3 mW and is held at this value until the end of the measurement. Force exerted on the bead (a) and integrated fluorescence (b, c, and d) of dye solution with a trapped SCS over time. In order to show only variations in the fluorescence intensity, we subtract the background signals observed for each interval of measurements with constant pump power. Rectangles denote the time intervals when the pump power was gradually changed.

Finally, Fig. 9 repeats the measurement of Fig. 7 but at a higher constant pump power (1.6 mW). A strong flash of emission was observed which has been observed in previous studies of SEF [14,23]. A sharp position shift of the SCS is also present which coincides with the flash, thus, further demonstrating the high correlation between the emission and probe recoil.

IV. DISCUSSION

A. Fluorescence recoil effect

In Fig. 3 the SCS already responds differently to the pump power than the SS in the absence of dye molecules. There are a few reasons that can be considered to explain this. The first is that resonance with surface plasmons of the metal increases the incident field and thus the radiation force. Second, these metal areas also increase the scattering force from

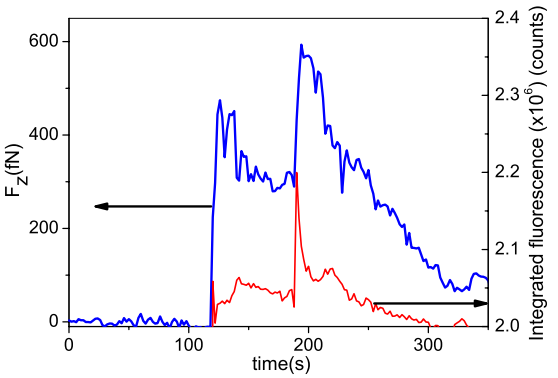

FIG. 9. (Color online) A flash of fluorescence intensity observed for the highest pump power (1.6 mW) used in the experiments. Measured integrated fluorescence (right axis) of dye solution with a trapped SCS plotted with the measured force z (left axis) on the bead over time. In this case, the pump is turned on to a much higher power than Fig. 7. A flash of emission is observed at 190 s.

the pump beam. In addition to scattering light, the silver colloids absorb the pump beam changing the absorption cross section of the SCS. Finally, this absorption could lead to an increase in temperature of the SCS and hence cause heat to be dissipated into the proximal surrounding liquid.

This last point, if true, would lead to a radiometric force [24] opposite to the temperature gradient within the particle. However, a temperature increase can be estimated from the given experimental conditions (max power of the pump beam at 3 mW; diameter of the pump beam around 1 μm) using a method described in [25–27]. If we assume that a metal island is a sphere with diameter of 100 nm, a dielectric susceptibility of silver (at 532 nm) to be $\epsilon=-10.187+i0.83$, and the thermal conductivity of water is 0.6 W/K m, then the calculation shows that the temperature increase is less than 10 °C relative to the temperature of the liquid. If we consider the 10% metal coverage of the sphere surface and also that the nanospheres are located on the surface of silica, a material with a greater thermal conductivity (1.3 W/K m) than water, then the temperature change cannot be more than this percentage of the total estimated increase, and so, the effect of these radiometric forces can be ruled out.

Although the SCS response varies based on the pump power it is important to realize that the force acting on this bead remains constant at a fixed power in the absence of dye. This is indeed observed in Fig. 4. The SCS shifts as the power is changed; however, it then remains at a stable position at the given pump power value. Thus, any additional temporal behavior of the measured force can be attributed to effects that are external to the bead.

The enhancing effect of the SCS can be seen when comparing Figs. 6 and 7. In the SS correlation, the plain silica bead simply expels dye molecules from the focal volume, thus decreasing the emitted fluorescence when the bead is trapped. The difference in the SCS is, of course, the addition of the silver nanocolloids to the surface of the bead. In this situation, there are now two sets of dye molecules: those that continue to diffuse in and out of the focal volume as before and those that adsorb or become fixed to the surface of the metal. For the former, dye molecules close enough to the

metal surfaces can still be enhanced due to the subnanometer to nanometer decay range of the enhancing electromagnetic field [8,9], but they avoid photobleaching due to the constant molecule replenishing in and out of the focal volume. For the latter, dye molecules naturally attach to the metal surfaces through adsorption processes or other attractive effects from the strong plasmon fields [28]. Although fluorescence quenching can occur for a single molecule adsorbed to a metal surface [9], enhanced fluorescence has been observed from ensemble measurements [8]. This is most likely due to molecules positioned adjacent to metals or molecular layering that would avoid the adsorbance-induced quenching but still keep the molecules fixed, thus still allowing photobleaching. In Fig. 7, the fluorescence is enhanced when the SCS is trapped and the bead responds by shifting away from its equilibrium position.

The fluorescence varies at the low constant power which is most likely due to the Brownian motion, both translational and rotational, of the SCS. This motion can alter areas of excitation at the bead surface which would vary the emitted fluorescence. This effect is more pronounced at low pump powers because the constant fluorescence background from the diffusing dye molecules is minimized allowing for the varying fluorescence to dominate. Conversely, the low power, and thus the lesser number of emitted photons, results in lower forces acting on the probe. The low forces are randomly countered by the probe Brownian fluctuations leading to an inconsistent correlation between the fluorescence and probe position, as seen in Fig. 7.

All changes in the fluorescence, no matter how small, can be attributed to interaction with the metal since the fluorescence intensity is constant in the absence of metal. Second, these fluorescence changes, seemingly small, should be considered in light of the large constant fluorescence from the nonenhanced diffusing dye molecules that is shown to be present in the SS measurement (Fig. 6).

At high pump powers, as demonstrated in Fig. 8, the probe once again experiences a force response to the enhanced emission. At these powers, the fluorescence signal is about two orders of magnitude higher that in Fig. 6. In addition, the photobleaching effect of the dye is revealed in both the integrated fluorescence and the force response of the probe. For the former, the percentage decrease in the fluorescence is 3%–5% of the *total* measured fluorescence from the focal volume which includes the large constant fluorescence background mentioned earlier. In addition, the photobleaching is less apparent because the effect occurs during the periods of pump power increase as well. Nevertheless, the SCS position responds by asymptotically decreasing toward its initial position that is slightly offset at each stage by the change in pump power. The rates of decrease of the fluorescence and recoil force both have tens of seconds time scales which is similar to the photobleaching lifetime of organic dyes such as Rhodamine 6G [29,30]. Similarly, a diminishing fluorescence and bead movement is observed after each power increase. This is another typical characteristic of photobleaching, where partially damaged molecules continue to emit light but at lower radiative rates. The difference in force between the final points of adjacent pump power intervals should be close to the radiation pressure force values of Fig. 3 for the SCS in the absence of dye. Figure 8 in fact seems to show that these values are lower. This is most likely due to the fact that the molecules on the surfaces, that are bleached or quenched, are still absorbing light; however, this incident energy is now being dissipated nonradiatively as heat rather than through the emission of photons. This does not affect the bead position, and since some of the incident light is now absorbing at a high loss, this explains why the asymptotic values of the optical force do not agree between Figs. 3 and 8. For the former, force values were taken rapidly and for the SCS in water, while for the latter, the bead was irradiated at each power for tens of seconds in dye solution.

An interesting phenomenon that is also observed with these surface plasmon enhancing probes is the random appearance of a short burst of light or "flash" in the measured emission. This has been previously observed for both SERS and SEF [14,23] with very little understanding of its origin. At high pump powers, the local highly intense fields at the metal surfaces can be enough to reconfigure the adsorbed molecule to metal structure orientation [31]. This could make it possible to have random moments of large resonances that would produce such a burst of light. We present our observation of this phenomenon in Fig. 9 only to demonstrate that the probe recoil can characterize these short time-scale fluorescence events as well; however, this flash is still an unexplained phenomenon.

B. Recoil effect as a probe

The current results are a confirmation and expansion of those of [6] in that this form of the PFM technique has now been shown to be applicable to more than one form of emission. SEF is still not a well understood process, similar to SERS, and this technique provides a secondary measure to the direct detection of the fluorescence emission. At the right experimental conditions, such as trap stiffness and optical alignment, the recoil of the trapped bead can provide another data point that is comparable to the detected emission itself. In addition, the measured probe recoil is capable of tracking the well-known photobleaching phenomenon in fluorescence. The example given here is the observance of bleaching through the reducing of the recoil of the bead over time at a fixed power. In this case, the changing bead position demonstrates the bleaching effect more clearly than the measured fluorescence.

An intriguing conclusion is that when using the PFM technique to study optical processes, where the light emission is measured from these trapped probes, there is a high sensitivity to effects on the probe surface at high pump powers. In this regime, the force is sensitive to photobleaching of dye molecules that could only come from those that are fixed to the metal surfaces. This could be a fortunate result due to the fact that the highest emission enhancement happens to molecules that are closest to the metal nanostructured surfaces [8,9], and thus, the probe would naturally be more sensitive to the dynamics of these molecules versus those that diffuse in and out of the focal volume. In the end, the probe force response is relatively insensitive to the large constant fluorescence background. Thus, it is able to resolve the

dynamic process of photobleaching as well as a measurement of the fluorescence itself.

Future work entails experimenting with different sized beads and other metals for the surface. However, the overall result is clear that the PFM technique is sensitive enough to be useful for the study of the entire range of light-matter interaction.

V. CONCLUSION

The momentum transfer from emitted fluorescence photons was studied by optically trapping a partially metal covered bead in the presence of dye molecules. The silver colloids create a surface-enhanced fluorescence that creates enough photons to observe a momentum transfer via a recoil of the trapped bead. The resulting position fluctuation data provide a measure complimentary to the detected emission that can be used to observe well-known photobleaching effects as well as possibly aid in elucidating lesser understood processes such as surface-enhanced emission from metal colloids.

ACKNOWLEDGMENTS

We thank M. P. Kreuzer and S. Balint for providing us the metal covered beads. We acknowledge support from MIIN Grant No. FIS2008-00114 (Spain) and Fundació Cellex Barcelona.

[1] J. D. Jackson, *Classical Electrodynamics*, 2nd ed. (Wiley, New York, 1975).
[2] C. F. Bohren and D. R. Huffman, *Absorption and Scattering of Light by Small Particles* (John Wiley and Sons, Inc., New York, 1983).
[3] A. Ashkin and J. M. Dziedzic, Phys. Rev. Lett. **38**, 1351 (1977).
[4] A. Fontes, A. A. R. Neves, W. L. Moreira, A. A. de Thomaz, L. C. Barbosa, C. L. Cesar, and A. M. de Paula, Appl. Phys. Lett. **87**, 221109 (2005).
[5] Y. Matsuo, H. Takasaki, J. Hotta, and K. Sasaki, J. Appl. Phys. **89**, 5438 (2001).
[6] S. Rao, S. Balint, P. Lovhaugen, M. Kreuzer, and D. Petrov, Phys. Rev. Lett. **102**, 087401 (2009).
[7] E. Fort and S. Gresillon, J. Phys. D **41**, 013001 (2008).
[8] K. Sokolov, G. Chumanov, and T. Cotton, Anal. Chem. **70**, 3898 (1998).
[9] P. Anger, P. Bharadwaj, and L. Novotny, Phys. Rev. Lett. **96**, 113002 (2006).
[10] J. R. Lakowicz and Yi Fu, Laser Photonics Rev. **3**, 221 (2009).
[11] J. Prikulis, F. Svedberg, M. Kall, J. Enger, K. Ramser, M. Goksor, and D. Hanstorp, Nano Lett. **4**, 115 (2004).
[12] F. Svedberg, Z. Li, H. Xu, and M. Kall, Nano Lett. **6**, 2639 (2006).
[13] L. Bosanac, T. Aabo, P. M. Bendix, and L. B. Oddershede, Nano Lett. **8**, 1486 (2008).
[14] G. McNay, F. T. Docherty, D. Graham, W. E. Smith, P. Jordan, M. J. Padgett, J. Leach, G. Sinclair, P. B. Monaghan, and J. M. Cooper, Angew. Chem. Int. Ed. **43**, 2512 (2004).
[15] P. Jordan, J. Cooper, G. McNay, F. T. Docherty, W. E. Smith, G. Sinclair, and M. J. Padgett, Opt. Lett. **29**, 2488 (2004).
[16] P. Jordan, J. Cooper, G. McNay, F. T. Docherty, D. Graham, W. E. Smith, G. Sinclair, and M. J. Padgett, Opt. Express **13**, 4148 (2005).
[17] Y. Saito, J. J. Wang, D. A. Smith, and D. N. Batchelder, Langmuir **18**, 2959 (2002).
[18] S. Nie and S. R. Emory, Science **275**, 1102 (1997).
[19] S. Balint, M. Kreuzer, S. Rao, G. Badenes, P. Miskovski, and D. Petrov, J. Phys. Chem. C (to be published).
[20] P. C. Lee and D. Meisel, J. Phys. Chem. **86**, 3391 (1982).
[21] M. A. Noginov, M. Vondrova, S. N. Williams, M. Bahoura, V. I. Gavrilenko, S. M. Black, V. P. Drachev, V. M. Shalaev, and A. Sykes, J. Opt. A, Pure Appl. Opt. **7**, S219 (2005).
[22] K. Berg-Sorensen and H. Flyvbjerg, Rev. Sci. Instrum. **75**, 594 (2004).
[23] A. Zhdanov, M. P. Kreuzer, S. Rao, A. Fedyanin, P. Ghenuche, R. Quidant, and D. Petrov, Opt. Lett. **33**, 2749 (2008).
[24] M. Lewittes, S. Arnold, and G. Oster, Appl. Phys. Lett. **40**, 455 (1982).
[25] H. Goldenberg and C. J. Thiele, Br. J. Appl. Phys. **3**, 296 (1952).
[26] Y. Seol, A. E. Carpenter, and T. T. Perkins, Opt. Lett. **31**, 2429 (2006).
[27] A. O. Govorov and H. H. Richardson, Nano Today **2**, 30 (2007).
[28] N. Calander and M. Willander, Phys. Rev. Lett. **89**, 143603 (2002).
[29] C. Eggeling, J. Widengren, R. Rigler, and C. A. M. Seidel, Anal. Chem. **70**, 2651 (1998).
[30] C. Eggeling, A. Volkmer, and C. A. M. Seidel, ChemPhysChem **6**, 791 (2005).
[31] A. Kudelski and B. Pettinger, Chem. Phys. Lett. **383**, 76 (2004).